J Mol Model (2016) 22: 144
DOI 10.1007/s00894-016-3011-3

ORIGINAL PAPER

Computer-aided rational design of novel EBF analogues with an aromatic ring

Shanshan Wang[1] · **Yufeng Sun**[2] · **Shaoqing Du**[1] · **Yaoguo Qin**[1] · **Hongxia Duan**[1] · **Xinling Yang**[1]

Received: 29 March 2016 / Accepted: 19 May 2016 / Published online: 1 June 2016

Abstract Odorant binding proteins (OBPs) are important in insect olfactory recognition. These proteins bind specifically to insect semiochemicals and induce their seeking, mating, and alarm behaviors. Molecular docking and molecular dynamics simulations were performed to provide computational insight into the interaction mode between AgamOBP7 and novel (*E*)-β-farnesene (EBF) analogues with an aromatic ring. The ligand-binding cavity in OBP7 was found to be mostly hydrophobic due to the presence of several nonpolar residues. The interactions between the EBF analogues and the hydrophobic residues in the binding cavity increased in strength as the distance between them decreased. The EBF analogues with an *N*-methyl formamide or ester linkage had higher docking scores than those with an amide linkage. Moreover, delocalized π–π and electrostatic interactions were found to contribute significantly to the binding between the ligand benzene ring and nearby protein residues. To design new compounds with higher activity, four EBF analogues **D1–D4** with a benzene ring were synthesized and evaluated based on their docking scores and binding affinities. **D2**, which had an *N*-methyl formamide group linkage, exhibited stronger binding than **D1**, which had an amide linkage. **D4** exhibited particularly strong binding due to multiple hydrophobic interactions with the protein. This study provides crucial foundations for designing novel EBF analogues based on the OBP structure.

Keywords EBF analogues · Odorant binding protein · Rational design · Semiochemicals · Insect behavior regulators

Electronic supplementary material The online version of this article (doi:10.1007/s00894-016-3011-3) contains supplementary material, which is available to authorized users.

✉ Hongxia Duan
hxduan@cau.edu.cn

✉ Xinling Yang
yangxl@cau.edu.cn

[1] Department of Applied Chemistry, College of Science, China Agricultural University, Beijing 100193, China

[2] Laboratory of Agro-products Quality Safety Risk Assessment, Institute of Agro-products Processing Science and Technology, Chinese Academy of Agricultural Sciences, Beijing 100193, China

Introduction

Aphids are a major agricultural pest because they not only directly damage the leaves of many cultivated plants via a sap-feeding mode but also indirectly impact plant growth through a virus-transmitting mode [1]. Most aphids release the aphid alarm pheromone when they are attacked by other species, so this semiochemical could be used to keep aphids away from crops to protect them. The active ingredient in the aphid alarm pheromone was identified as (*E*)-β-farnesene (EBF) [2]. It is well known that EBF is unstable because of its multiple double bonds, which are easily oxidized in the environment. Therefore, EBF has been modified continually in recent years to develop novel EBF analogues. In particular, the EBF conjugated double bond has been modified in several studies (Fig. 1). An early study by Dawson et al. reported that some EBF analogues in which a few double bonds in the middle or terminal position were removed had better repellent responses [3]. EBF analogues without a terminal conjugated double bond were also found to exhibit good repellent activity by Li et al. [4]. At the same time, dimers of EBF analogues exhibited good alarm responses to peach aphids when the terminal conjugated double bonds in both EBF analogues were hydrogenated [5]. Recently, the EBF conjugated double bond was replaced with heteroatoms or heterocyclics, and Yang et al. synthesized approximately 200 new EBF

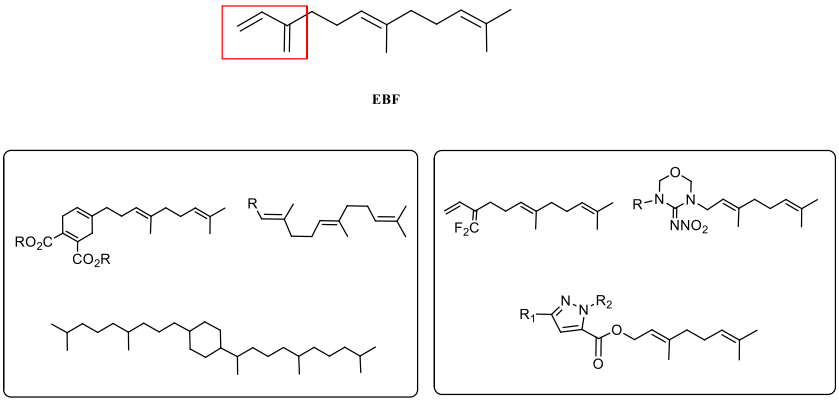

Fig. 1 The aphid alarm pheromone EBF and some of its analogues. EBF analogues synthesized by other groups and by our group are shown in the *left and right boxes*, respectively

analogues [6–10]. Many EBF analogues with an oxadiazine or pyrazole ring were found to have excellent repellent responses to aphids [7, 8].

It is well known that odorant binding proteins (OBPs) can bind specifically to insect semiochemicals to activate their seeking, mating, and alarm behaviors. Therefore, OBPs have become an interesting potential target in attempts create new insect behavior regulators in recent years, and the binding between some OBPs in aphids and EBF has received particular attention [11–13]. Pelosi et al. reported that ApisOBP3 is involved in the detection and recognition of EBF, which exhibits a high binding affinity to it [13]. SaveOBP7 in *Hemiptera* species was also found to play an important role in EBF recognition [14]. Recently, ApisOBP7 was proposed by Yang et al. to bind specifically not only to EBF but also to its analogues with a pyrazole ring [15]. More importantly, some EBF analogues with high binding affinities surprisingly exhibited good repellent responses to aphids [15]. Moreover, OBP, which is an important protein in insect olfactory recognition, could transfer the bound ligand to downstream olfactory receptors (ORs) to further stimulate insect behavioral responses. If OBP and OR constitute a two-step filter, OR would be another potential target in attempts to control insect behavior by olfactory perception because OBP and OR share a common ligand [16]. However, studies of the binding between OR and the ligand are currently still limited.

Increasing attention has recently focused on ligand–protein interactions. Recently, the crystal structures of insect OBP1, OBP7, OBP4, and OBP14 were successfully solved, and they could stimulate new research on novel insect behavioral controls based on OBPs [16–21]. Surprisingly, in our previous work, some EBF analogues with a pyrazole or benzene ring were found to exhibit not only good binding affinity to ApisOBP7 but also good repellent responses to aphids [15]. However, the interaction mechanism between these EBF analogues and OBP7 is unknown, and it is unclear if new analogues can be designed based on the OBP7 binding cavity. Therefore, the interaction mode between OBP7 and EBF analogues with an aromatic ring was investigated by molecular docking and molecular dynamics simulations in this study. Moreover, new EBF analogues were designed and synthesized based on the determined ligand–protein interaction mode. This study provides significant guidance for the design of novel EBF analogues based on OBPs.

Materials and methods

In our previous work, twelve EBF analogues with a pyrazole or benzene ring were synthesized [8, 15], and their binding affinities to ApisOBP7 were measured by recording the fluorescence peak values of different EBF analogues and *N*-phenyl-1-naphthylamine (1-NPN) during their competitive binding to the protein [13, 22]. However, the interaction mode between these EBF analogues and ApisOBP7 was not clear. To our knowledge, no ApisOBP7 crystal structure has been reported to date. AgamOBP7 complexed with a palmitic acid (PA) (PDB code: 3R1P) shares a certain sequence identity with ApisOBP7 (Fig. S1 in the "Electronic supplementary material," ESM) and co-crystallizes with a long linear ligand (PA) similar to EBF [19]. More importantly, AgamOBP7 has a hydrophobic, elongated, and open binding cavity similar to that of the ApisOBP7 model (Fig. S2 in the ESM) surrounded by nearly the same nonpolar residues (Table S1 in the ESM) [23]. This binding cavity can accommodate elongated linear ligands similar to EBF analogues (Fig. S3 in the ESM) [19]. Therefore, twelve EBF analogues were docked into AgamOBP7 as a model for ApisOBP7 using the Surflex-Dock software to explore the binding mode. The docking results for PA, EBF, and its **I-5** and **D-4** analogues were verified by 20-ns molecular dynamics simulations, which were performed using the GROMACS 4.0.5 package [24, 25]. The G43a1 force field was used to calculate the protein energy, and the topology files and force-field parameters of the ligand were generated using the PRODRG program [26]. Each complex was solvated with explicit solvent (SPC) water and neutralized by adding 6 Na^+ ions. The steepest-descent and conjugated-gradient methods were used to minimize the energy of each system. The reference temperature was fixed at 300 K, and all bonds were constrained with LINCS [27].

Long-range electrostatics was handled using PME during each simulation [28]. Unless otherwise specified, OBP7 actually refers to AgamOBP7 in this study. The initial conformations of all the EBF analogues were optimized at the B3LYP/6-31G level in Gaussian 03 [29]. The Protomol based on the ligand mode was generated as the ligand binding pocket. The docking score represents the ligand binding affinity to the protein, which is usually correlated to the ligand pIC_{50} value [30, 31]. It is well known that Surflex-Dock is an accurate, rapid, and efficient tool for protein-ligand binding simulations, and is especially successful at eliminating false-positive results [32]. This software has become a commercial module in the SYBYL software package [33]. A prototype molecule algorithm was employed in Surflex-Dock, and ligand flexibility was considered in the docking process [30]. Four new EBF analogues were designed based on the interaction mode between the known EBF analogues and OBP7, and were then synthesized according to Scheme 1. The binding affinities (IC_{50} values) were measured by recording the fluorescence peak values of the four EBF analogues and 1-NPN during competitive binding to ApisOBP7. The protein was prepared and purified according to previously reported procedures [13].

Results and discussion

Difference between the binding modes of pyrazole-substituted EBF analogues with ester and amide linkages

Although the OBP7 binding cavity was reported to be flexible and adaptable [19], EBF acted as a good regulator, like native

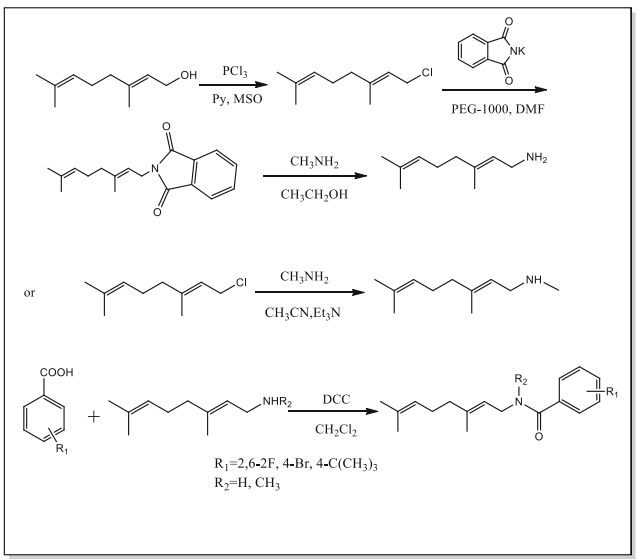

Scheme 1 Synthesis route for the newly designed EBF analogues **D1–D4**

PA, stabilizing the OBP7 protein during the whole docking process, as confirmed by the 20-ns MD results (Fig. S4 in the ESM). The results clearly showed that the OBP7 binding cavity was suitable for binding the linear EBF analogues. Twelve EBF analogues with an aromatic ring [8] were docked into OBP7 to determine their binding modes. The obtained docking scores of all the EBF analogues are given in Table 1. The scores of compounds **I-1**, **II-1**, **I-2**, and **II-2** in group A correlated well with the binding affinities (pIC_{50} values), with a high coefficient of 0.96 (Fig. S5 in the ESM). As shown in Fig. 2a, the ligand binding cavity in OBP7 was found to be a long, narrow hydrophobic tunnel with several nonpolar residues (Phe120, Leu124, Val125, and Val117) along the top and some hydrophobic residues (Leu72, Ile57, Phe54, Leu53, Ile50, and Val107) along the bottom [19]. It is similar to the ApisOBP7 model binding domain with the hydrophobic residues Phe52, Ile109, Leu57, and Val88 [23], which also has the same residues as the ApisOBP3 model except for Tyr84 [13]. A similar inner hydrophobic cavity was also found in the SlitOBP1 model [34]. Figure 2b shows that **I-1** and **II-1**, which have ester and amide linkages, respectively, both fit into the long hydrophobic OBP7 cavity well. However, the **I-1** molecule was better accommodated in the hydrophobic pocket—it had a higher clogP value (6.34) than that of **II-1** (5.34). This explained why the score and binding affinity of **I-1** were better than those of **II-1**. As indicated in Table 1, when the methyl group on the pyrazole ring in **I-1** and **II-1** was replaced with a bulky propyl group to give **I-2** and **II-2**, respectively, the docking scores decreased. Steric hindrance caused **I-2** and **II-2** to move outside the binding domain, where they could not interact with the hydrophobic residues in the binding cavity. These results are consistent with previous reports suggesting that the presence of a short chain on the pyrazole ring enhances the binding affinity of EBF analogues [23]. In short, the size of the hydrophobic group could be an important consideration when modifying EBF to optimize its contacts with protein residues in the OBP7 binding domain.

Binding modes of the pyrazole-substituted EBF analogues with an *N*-methyl formamide or amide linkage

As shown in Table 1, the docking scores of the pyrazole-substituted EBF analogues **III-1**, which has an *N*-methyl formamide linkage, and **II-3**, which has an amide linkage, were similar. As shown in Fig. 3a, both **III-1** and **II-3** of group B could be accommodated in the hydrophobic OBP7 binding region. As shown in Fig. 3b, part of **II-4** was located outside the narrow entrance of the protein binding pocket because of the bulky isopropyl group. In addition, the amide group in **II-4** formed a weak H-bond with the carbonyl of the hydrophilic Leu53 residue, preventing its entry into the binding cavity. Therefore, the **II-4** docking score was lower than the other

Table 1 Structures, docking scores, and binding affinities of the EBF analogues with an aromatic ring

No.	Structure	Score [a]	IC_{50} (μM) [b]	pIC_{50}
I-1	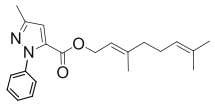	7.06	2.8	5.55
I-2	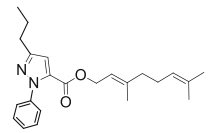	6.69	6.8	5.17
I-3	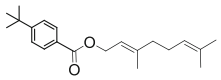	7.95	3.0	5.52
I-4	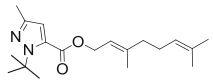	6.64	4.8	5.32
I-5	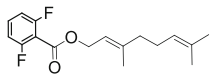	8.22	1.3	5.89
I-6	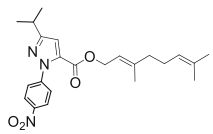	7.51	3.6	5.44
II-1	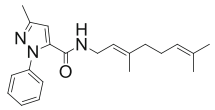	6.38	9.3	5.03
II-2	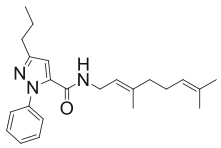	6.05	14.1	4.85
II-3	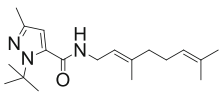	7.82	8.2	5.09
II-4	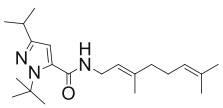	7.69	11	4.96
III-1	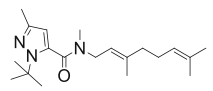	7.91	5.1	5.29
III-2	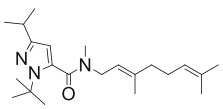	7.86	5.3	5.28

[a] docking score for binding to AgamOBP7

[b] binding affinity to ApisOBP7

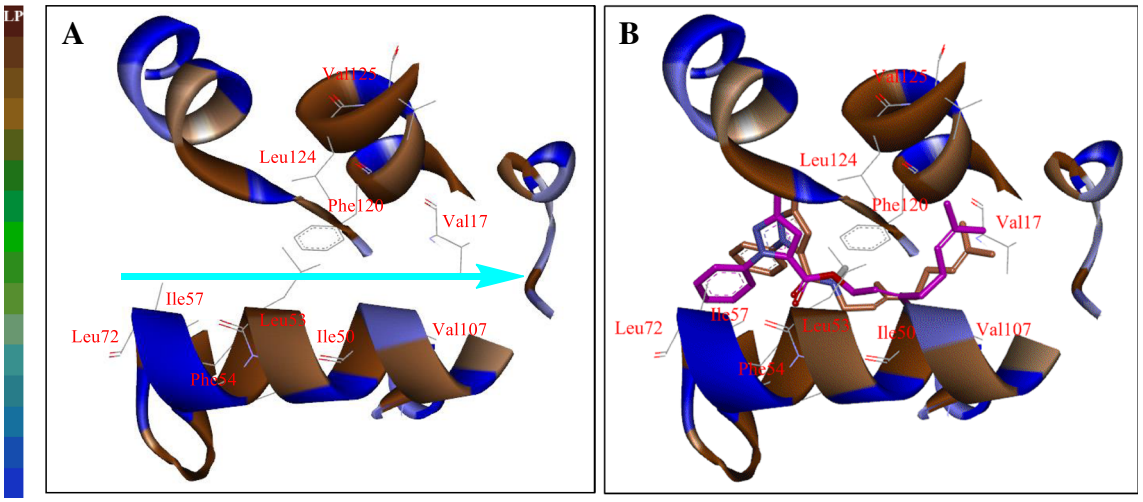

Fig. 2a–b OBP7 binding cavity and the interaction modes between different ligands and OBP7. **a** Long, narrow hydrophobic binding cavity in OBP7. The inner helix surface, which has some hydrophobic residues, is shown in *brown*, and the external helix surface, which has some hydrophilic residues, is shown in *blue*. The key residues in the OBP7 binding cavity are labeled with a three-letter ID and depicted using a *line model*. **b** Alignment of compounds **I-1** (*magenta*) and **II-1** (*tan*) in the OBP7 binding cavity. The long chain of each EBF analogue is well matched with the long hydrophobic OBP7 cavity

docking scores. However, in a previous study, the binding affinities of **III-1** and **III-2**, which have an *N*-methyl formamide group, were found to be higher than those of **II-3** and **II-4**, respectively, which have an amide group, based on the binding assay results [15]. The results of this study can be explained by the hydrophobicity of **III-1** and **III-2**, which enabled them to penetrate into the cell membrane more easily. In short, hydrophobic interactions are very important for the binding between these pyrazole-substituted EBF analogues and OBP7. Some hydrophobic side chains could be included on the EBF long chain to improve its hydrophobic interactions with OBP.

Binding affinity analysis for EBF analogues with different aromatic rings

Because an ester group was previously used as a linkage between EBF and a pyrazole ring, analogues with an ester group linkage between EBF and a different aromatic benzene ring were studied [23]. Molecular docking simulations were used to provide insight into the binding mode between OBP7 and these EBF analogues, which constitute group C.

As shown in Table 1, the binding affinities and docking scores of compounds **I-3** and **I-5** with benzene rings were significantly higher than those of **I-4** and **I-6** with pyrazole rings. As shown in Fig. 4a, **I-3** with a benzene ring could be

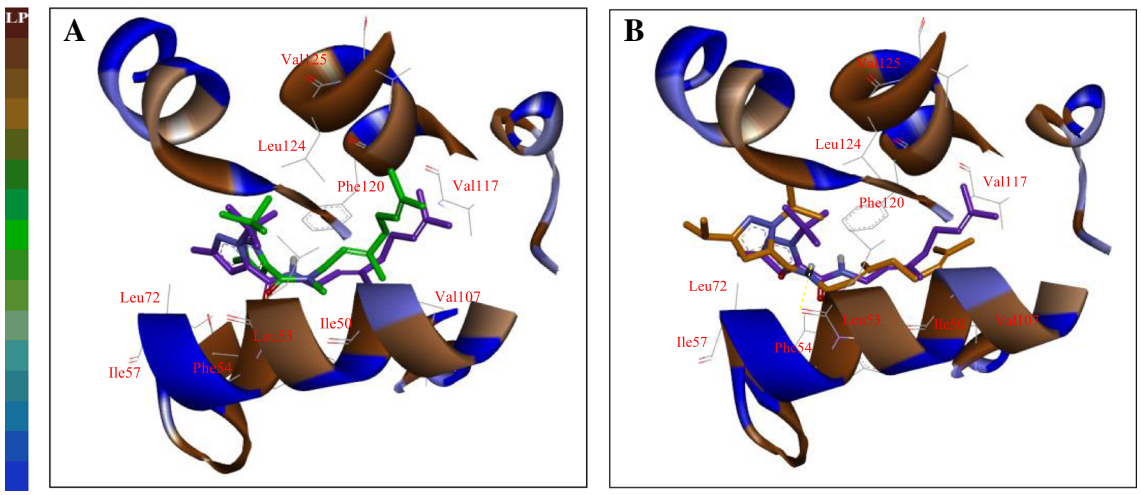

Fig. 3a–b Hydrophobic interactions between different EBF analogues and OBP7. **a** Compounds **III-1** (*green*) and **II-3** (*purple*). **b** Compounds **II-3** (*purple*) and **II-4** (*orange*). The inner helix surface, which has some hydrophobic residues, is shown in *brown*, and the external helix surface, which has some hydrophilic residues, is shown in *blue*. The key residues in the OBP7 binding cavity are labeled with a three-letter ID and depicted using a *line model*

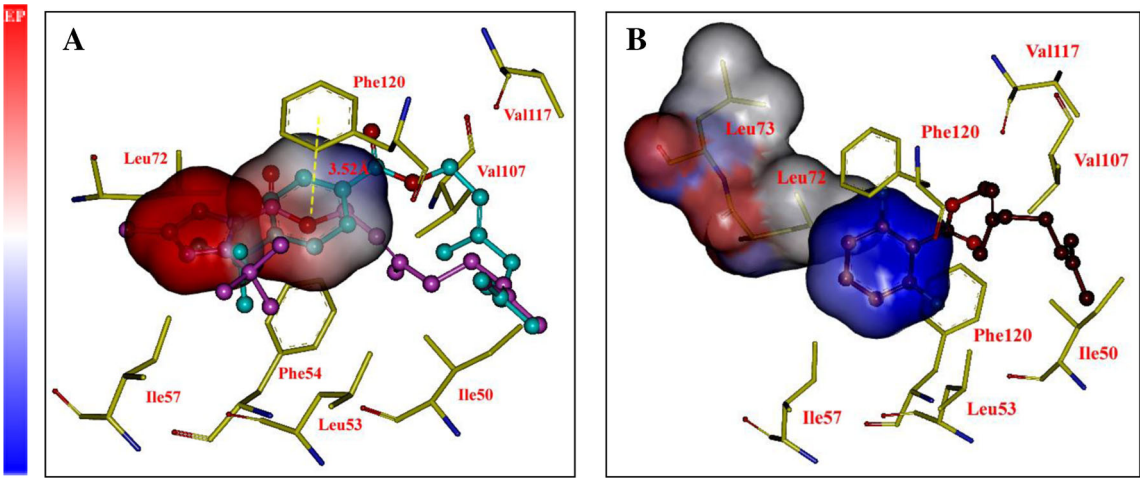

Fig. 4a–b Electrostatic interactions between different EBF analogues and OBP7. **a** Compounds **I-3** (*light blue*) and **I-4** (*pink*) in the OBP7 binding domain. The potentials on the **I-3** benzene ring and **I-4** pyrazole ring are positive (*blue*) and negative (*red*), respectively. (**b**) Electrostatic interactions between compound **I-5** (*crimson*) and OBP7. The positive potential (*blue*) on the **I-5** benzene ring interacts with the negative potential (*red*) on OBP7 residues Leu72 and Leu73

accommodated in the binding domain and formed strong contacts with the surrounding hydrophobic OBP7 residues. Moreover, delocalized electrons on the **I-3** benzene ring resulted in a positive electrostatic potential surface, whereas the electrostatic potential of the **I-4** pyrazole ring was negative (Fig. 4a). The **I-3** benzene ring formed a π–π stacking interaction with residue Phe120 of OBP7 at a distance of only 3.52 Å. These results could explain those of a previous work which noted that replacing the EBF conjugated double bond with a benzene ring led to desirable binding properties [23]. In that study, only a few of the EBF analogues were tested for repellent activity, and aphids were found to have a repellent response to **I-3**, which exhibited a good binding affinity IC_{50} value of 3.0 μM [23]. It was clear that not only did hydrophobic interactions contribute to the binding affinity of EBF analogues to OBP7, but an additional π-electron effect was also beneficial for the binding [35, 36].

In addition to the hydrophobic *t*-butyl substituent on the benzene ring of the EBF analogue **I-3**, electron-withdrawing F substituents were placed on the benzene ring of the EBF analogue **I-5**. The binding assays indicated that **I-5** with two F atoms had a much higher binding affinity with an IC_{50} value of 1.3 μM, as shown in Table 1 [23]. It also had a higher docking score of 8.22, as confirmed by a 20-ns MD simulation (Fig. S6 in the ESM). These results can be explained by the fact that the electron-withdrawing F atoms greatly increased the electropositive potential of the **I-5** benzene ring, which could induce electrostatic interactions with several nearby OBP7 residues, especially Leu72 and Leu73, as shown in Fig. 4b. Thus, substituting the EBF conjugated double bond with an aromatic benzene ring was clearly beneficial for improving the binding. Moreover, including some electron-withdrawing groups on the benzene ring of each EBF analogue also enhanced the binding by increasing the electrostatic interactions.

Newly designed EBF analogues based on the OBP7 binding cavity

Using an *N*-methyl formamide group as the linkage was shown to increase the hydrophobic contacts between EBF analogues and OBP7, thereby improving their binding. Moreover, electron delocalization over the EBF analogue benzene ring was also found to enhance the protein–ligand binding. Therefore, four new EBF analogues were designed and synthesized with a benzene ring and an *N*-methyl formamide linkage or amide linkage as a control in this study (Scheme 1). They were denoted **D1**–**D4** of group D, and their binding affinities and docking scores were calculated to provide insight into their abilities to bind to OBP7. The results are listed in Table 2.

As shown in Table 2 and Fig. S5 of the ESM, the docking scores of newly designed EBF analogues **D1**–**D4** were well correlated with their binding affinities (pIC_{50}). The binding affinities and docking scores of **D1** and **D2** (Table 2) were found to be much lower than those of **I-5** (Table 1). Clearly, when the EBF conjugated double bond was replaced with a benzene ring with two F atoms, the binding abilities of analogues with different linkages decreased as follows: ester > *N*-methyl formamide > amide. Increasing the hydrophobicity of the linkage, by using an ester group for instance, enabled stronger hydrophobic interactions between the EBF analogues and the OBP7 binding domain, as discussed previously. To further evaluate the effect of the substituent position on the benzene ring, a Br atom was placed in the position para to the EBF long chain to synthesize **D3**. Its binding affinity (IC_{50} = 3.3 μM) was slightly higher than that of **D2** (IC_{50} = 6.0 μM) (Table 2). The para substituent on the benzene ring might have enabled the EBF analogues to fit into the long, narrow OBP7 binding cavity better.

Table 2 Structures, docking scores, and binding affinities of the newly synthesized EBF analogues

No.	Structure	Score [a]	IC_{50} (μM) [b]	pIC_{50}
D1	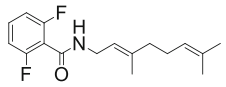	7.20	8.5	5.07
D2	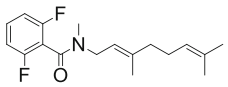	7.63	6.0	5.22
D3	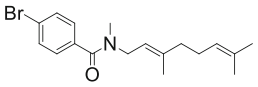	8.09	3.3	5.48
D4	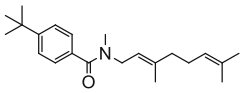	8.41	1.7	5.77

[a] docking score for binding to AgamOBP7

[b] binding affinity to ApisOBP7

As discussed previously, the EBF analogues with an ester linkage were found to exhibit stronger binding than those with an *N*-methyl formamide linkage. Because the protein binding cavity had a long, narrow hydrophobic channel, a new EBF analogue with a *t*-butyl substituent on the benzene ring and an *N*-methyl formamide linkage was designed, synthesized, and denoted **D4**. Surprisingly, the binding affinity of **D4** was high, with an IC_{50} value of 1.7 μM (Table 2), which was close to the IC_{50} value of the known **I-5** analogue (Table 1). As shown in Fig. 5a and confirmed by a 20-ns MD simulation (Fig. S6), **D4** was closely surrounded by key hydrophobic residues in the OBP7 binding cavity. The hydrophobic *t*-butyl group in **D4** interacted with the hydrophobic Leu72 and Ile57 residues at the binding pocket entrance. In contrast, as shown in Fig. 5b, the electron-withdrawing F atoms in **I-5** greatly increased the electropositive potential of the benzene ring, inducing electrostatic interactions with nearby polar protein residues such as Leu53. Moreover, the *N*-methyl formamide linkage in **D4** led to a higher binding affinity to the protein than the ester linkage in **I-3**. The methyl group on the **D4** *N*-methyl formamide fragment provided an additional contact point in the hydrophobic binding cavity. Similarly to **I-3**, **D4** also formed a π–π

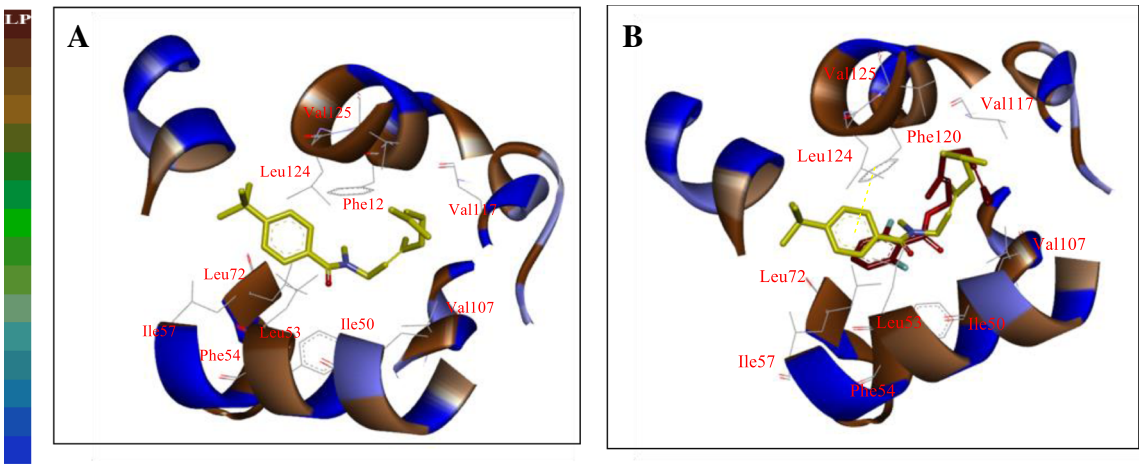

Fig. 5a–b Binding modes between the newly synthesized EBF analogues and OBP7. **a** Hydrophobic interactions between OBP7 and **D4**, which had a high binding affinity. The **D4** docking conformation fitted well into the OBP7 hydrophobic binding cavity. **b** Alignment of the newly synthesized **D4** (*yellow*) and the reported **I-5** (*crimson*) in the OBP7 binding cavity. The conformation of **D4** in the OBP7 binding cavity was narrower, whereas one of the **I-5** F atoms interacted with the polar Leu53 residue of OBP7

interaction with the nonpolar Phe120 residue in the protein binding domain. Clearly, the hydrophobic interactions were dominant in the binding between the EBF analogues and OBP7 because its binding domain is a long, narrow hydrophobic tunnel. In addition, electronic effects were also proposed to strengthen the binding between the EBF conjugated double bond or aromatic ring and nearby OBP7 residues.

Conclusions

Molecular docking and molecular dynamics simulations of EBF analogues in the OBP7 binding cavity were performed to provide insight into the intermolecular binding mode and thus facilitate the design of novel EBF analogues with higher stability than EBF. Newly designed and synthesized compound **D4**, which had a *t*-butyl-substituted benzene ring and *N*-methyl formamide linkage, exhibited good binding affinity and had a high docking score because of multiple hydrophobic interactions with OBP7. The docking scores and binding affinities of the known pyrazole-substituted EBF analogues with an *N*-methyl formamide or ester linkage were higher than those of the analogues with an amide linkage. When the unstable conjugated double bond of EBF was replaced with a benzene ring, the binding affinity and docking score increased due to an additional π–π interaction between the delocalized electrons on the benzene and nearby protein residues. Substituting two electron-withdrawing F atoms on the benzene ring further delocalized the electrons, leading to electrostatic interactions and thus a significant increase in the binding affinity to the protein. Therefore, because the OBP7 binding cavity is hydrophobic, EBF analogues should first be modified with hydrophobic groups to increase the hydrophobic contact area between the ligand and protein binding tunnel. In addition, electron delocalization over the conjugated double bond or aromatic ring in each EBF analogue should strengthen the binding by increasing its electrostatic interactions with the protein. This study provides an insight that should aid the future development of new stable EBF analogues with good binding affinities based on the OBP structure.

Acknowledgments We thank Dr. Pelosi for fruitful discussions and writing assistance. This work was supported by the National Scientific and Technology Supporting Program of China (2011BAE06B05-5) and the National Natural Science Foundation of China (21132003, 31371946).

Author contributions S.S. Wang, S.Q. Du, and H.X. Duan conceived and designed the experiments. Y.F. Sun, Y.G. Qin, and X.L. Yang prepared the EBF analogues. S.S. Wang, Y.F. Sun, and H.X. Duan analyzed the data. S.S. Wang and H.X. Duan wrote the first draft of the manuscript. H.X. Duan and X.L. Yang made critical revisions and approved the final manuscript. All the authors reviewed and approved the final manuscript. The authors declare no conflict of interest.

References

1. Harris KF, Maramorosch K (1977) Aphids as virus vectors. Academic, New York, 4:435–454
2. Bowers WS, Nault LR, Webb RE, Dutky SR (1972) Aphid alarm pheromone: isolation, identification, synthesis. Science 177:1121–1122
3. Dawson GW, Giffiths DC, Pickett JA, Plumb RT, Woodcock CM, Zhang ZN (1988) Structure–activity studies on aphid alarm pheromone derivatives and their field use against transmission of barley yellow dwarf virus. Pestic Sci 22:17–30
4. Li ZM, Wang TS, Yao EY (1987) Researches on insect pheromone III studies on aphid alarm pheromone mimics. Acta Chem Sin 45: 1124–1128
5. Zhang ZN, Liu X, Pickett JA (1988) Several aphids alarm pheromone analogues possessing biological activity. Acta Entomol Sin 31:435–438
6. Sun L, Ling Y, Wang C, Sun YF, Rui CH, Yang XL (2011) Synthesis and biological activity of *E*-β-farnesene analogues containing substituent nitroguanidine. Chin J Org Chem 31:2061–2066
7. Kang TN, Ling Y, Rui CH, Yang XL, Fan XL, Chen FH (2008) Synthesis of *E*-β-farnesene analogues containing five-membered azaheterocycles and their biological activity. Chin J Org Chem 28:617–621
8. Sun YF, Li YQ, Ling Y, Yu HL, Yang SX, Yang XL (2011) Design, synthesis and biological activity of *E*-β-farnesene analogues containing pyrazole-carboxamide. Chin J Org Chem 31:1425–1432
9. Sun L (2013) Synthesis process and structure optimization of EBF analogue CAU1204. PhD dissertation. China Agricultural University, Beijing
10. Liu SH (2014) Design, synthesis and bioactivity of neonicotinoids and EBF analogues. PhD dissertation. China Agricultural University, Beijing
11. Pelosi P, Zhou JJ, Ban LP, Calvello M (2006) Soluble proteins in insect chemical communication. Cell Mol Life Sci 63:1658–1676
12. Tegoni M, Campanacci V, Cambillau C (2004) Structural aspects of sexual attraction and chemical communication in insects. Trends Biochem Sci 29:257–264
13. Qiao HL, Tuccori E, He XL, Gazzano A, Field L, Zhou JJ, Pelosi P (2009) Discrimination of alarm pheromone (*E*)-β-farnesene by aphid odorant-binding proteins. Insect Biochem Mol 39:414–419
14. Zhong T, Yin J, Deng SS, Li KB, Cao YZ (2012) Fluorescence competition assay for the assessment of green leaf volatiles and *trans*-β-farnesene bound to three odorant-binding proteins in the wheat aphid *Sitobion avenae* (Fabricius). J Insect Physiol 58:771–781
15. Sun YF, Qiao HL, Ling Y, Yang SX, Rui CH, Pelosi P, Yang XL (2011) New analogues of (*E*)-β-farnesene with insecticidal activity and binding affinity to aphid odorant-binding proteins. J Agric Food Chem 59:2456–2461
16. Tsitsanou KE, Thireou T, Drakou CE, Koussis K, Keramioti MV, Leonidas DD, Eliopoulos E, Iatrou K, Zographos SE (2012) *Anopheles gambiae* odorant binding protein crystal complex with the synthetic repellent DEET: implications for structure-based design of novel mosquito repellents. Cell Mol Life Sci 69:283–297
17. Mao Y, Xu XZ, Xu W, Ishida Y, Leal WS, Ames JB, Clardy J (2010) Crystal and solution structures of an odorant-binding protein from the southern house mosquito complexed with an oviposition pheromone. Proc Natl Acad Sci USA 107:19102–19107
18. Leite NR, Krogh R, Xu W, Ishida Y, Iulek J, Leal WS, Oliva G (2009) Structure of an odorant-binding protein from the mosquito *Aedes aegypti* suggests a binding pocket covered by a pH-sensitive "lid". PLoS ONE 4:e8006
19. Lagarde A, Spinelli S, Tegoni M, He XL, Field L, Zhou JJ, Cambillau C (2011) The crystal structure of ordorant binding protein 7 from *Anopheles gambiae* exhibits an outstanding adaptability of its binding site. J Mol Biol 414:401–412

20. Davrazou F, Dong E, Murphy EJ, Johnson HT, Jones DNM (2011) New insights into the mechanism of odorant detection by the malaria-transmitting mosquito *Anopheles gambiae*. J Biol Chem 286:34175–34183
21. Spinelli S, Lagarde A, Iovinella I, Legrand P, Tegoni M, Pelosi P, Cambillau C (2012) Crystal structure of *Apis mellifera* OBP14, a C-minus odorant-binding protein, and its complexes with odorant molecules. Insect Biochem Mol Biol 42:41–50
22. Sun YF, De Biasio F, Qiao HL, Iovinella I, Yang SX, Ling Y, Riviello L, Battaglia D, Falabella P, Yang XL, Pelosi P (2012) Two odorant-binding proteins mediate the behavioural response of aphids to the alarm pheromone (*E*)-β-farnesene and structural analogues. PLoS ONE 7(3):e32759
23. Sun YF (2011) Discovery of novel aphid control agents based on OBPs: design, synthesis and bioactivity of EBF analogues. PhD dissertation. China Agricultural University, Beijing
24. Hess B, Kutzner C, van der Spoel D, Lindahl E (2008) GROMACS4: algorithms for highly efficient, load-balanced, and scalable molecular simulation. J Chem Theory Comput 4:435–447
25. Berendsen HJC, van der Spoel D, van Drunen R (1995) GROMACS: a message-passing parallel molecular dynamics implementation. Comput Phys Commun 91:43–56
26. Schüttelkopf AW, van Aalten DMF (2004) PRODRG: a tool for high-throughput crystallography of protein–ligand complexes. Acta Crystallogr D 60:1355–1363
27. Hess B, Bekker H, Berendsen HJC, Fraajie JGEM (1997) LINCS: a linear constraint solver for molecular simulations. J Comput Chem 18:1463–1472
28. Essman U, Perela L, Berkowitz ML, Darden T, Lee H, Pedersen LG (1995) A smooth particle mesh Ewald potential. J Chem Phys 103: 8577–8592
29. Frisch MJ, Trucks GW, Schlegel HB, Scuseria GE, Robb MA, Cheeseman JR, Montgomery JA Jr, Vreven T, Kudin KN, Burant JC, Millam JM, Iyengar SS, Tomasi J, Barone V, Mennucci B, Cossi M, Scalmani G, Rega N, Petersson GA, Nakatsuji H, Hada M, Ehara M, Toyota K, Fukuda R, Hasegawa J, Ishida M, Nakajima T, Honda Y, Kitao O, Nakai H, Klene M, Li X, Knox JE, Hratchian HP, Cross JB, Bakken V, Adamo C, Jaramillo J, Gomperts R, Stratmann RE, Yazyev O, Austin AJ, Cammi R, Pomelli C, Ochterski JW, Ayala PY, Morokuma K, Voth GA, Salvador P, Dannenberg JJ, Zakrzewski VG, Dapprich S, Daniels AD, Strain MC, Farkas O, Malick DK, Rabuck AD, Raghavachari K, Foresman JB, Ortiz JV, Cui Q, Baboul AG, Clifford S, Cioslowski J, Stefanov BB, Liu G, Liashenko A, Piskorz P, Komaromi I, Martin RL, Fox DJ, Keith T, Al-laham MA, Peng CY, Nanayakkara A, Challacombe M, Gill PMW, Johnson B, Chen W, Wong MW, Gonzalez C, Pople JA (2003) Gaussian03, revision D.01. Gaussian, Inc., Wallingford
30. Jain AN (2003) Surflex: fully automatic flexible molecular docking using a molecular similarity-based search engine. J Med Chem 46: 499–511
31. Jain AN (1996) Scoring noncovalent protein–ligand interactions: a continuous differentiable function tuned to compute binding affinities. J Comput Aided Mol Des 10:427–440
32. Kellenberger E, Rodrigo J, Muller P, Rognan D (2004) Comparative evaluation of eight docking tools for docking and virtual screening accuracy. Proteins 57:225–242
33. Tripos Associates (2006) Sybyl version 7.3. Tripos Associates, St. Louis
34. Yi X, Zhang YB, Wang PD, Qi JW, Hu MY, Zhong GH (2015) Ligands binding and molecular simulation: the potential investigation of a biosensor based on an insect odorant binding protein. Int J Biol Sci 11:75–87
35. Salonen LM, Ellermann M, Diederich F (2011) Aromatic rings in chemical and biological recognition: energetics and structures. Angew Chem Int Ed 50:4808–4842
36. Janiak C (2000) A critical account on π–π stacking in metal complexes with aromatic nitrogen-containing ligands. J Chem Soc Dalton Trans 21:3885–389